

Low-temperature thermodynamic properties of a random anisotropic antiferromagnetic chain*

Jorge E. Hirsch[†]

*The James Franck Institute and Department of Physics,
University of Chicago, Chicago, Illinois 60637*

(Received 9 May 1980)

The low-temperature thermodynamic properties of a spin- $\frac{1}{2}$ one-dimensional random anisotropic (Heisenberg-Ising) antiferromagnet described by the Hamiltonian $H = \sum_i J_i (\sigma_x^i \sigma_x^{i+1} + \sigma_y^i \sigma_y^{i+1} + \gamma \sigma_z^i \sigma_z^{i+1})$ are studied as a function of disorder and anisotropy. The $J_i \geq 0$ are independent random variables obeying a probability distribution $P(J)$, and $0 \leq \gamma \leq \infty$. The approach used is a numerical implementation of a real-space renormalization-group (RG) method previously introduced. The isotropic Heisenberg case ($\gamma = 1$), the XY case ($\gamma = 0$), and the Ising case ($\gamma = \infty$) are fixed points of the RG transformation. It is found that in the XY region $\gamma \leq 1$, including the Heisenberg point, the system exhibits singular behavior in the thermodynamic properties for arbitrary probability distributions for the couplings. For the XY limit ($\gamma = 0$) this is in agreement with known exact results. The functional form for the low-temperature susceptibility is found to be $\chi \sim 1/(T \ln^m(T/T_0))$ in the entire region $0 \leq \gamma \leq 1$ for arbitrary probability distributions. In the Ising region ($\gamma > 1$) the susceptibility shows an approximate power-law divergence for small anisotropy but goes eventually to zero as $T \rightarrow 0$. Possible relevance of these results to recent experiments on Qn(TCNQ)₂ is discussed.

I. INTRODUCTION

In a previous paper¹ (hereafter referred to as I) the low-temperature thermodynamic properties of a random antiferromagnetic Heisenberg chain ($S = \frac{1}{2}$) were studied via an approximate renormalization-group (RG) technique. The results obtained were in striking contradiction with previous work on this model^{2,3}: The antiferromagnetic Heisenberg chain was found to display singular behavior in the low-temperature thermodynamic properties for *any form* of randomness present. An independent study by Ma *et al.*⁴ found similar results, while previous work had suggested that singular behavior would only be obtained if the underlying probability distribution for the couplings, $P(J)$, was singular at the origin (as happens in the classical Heisenberg-chain model.⁵

As pointed out earlier by Bulaevskii *et al.*⁶ however, our results could be expected since there exists a related model for which similar results are known to be exact. For the quantum XY model, an exact solution by Dyson⁷ for a certain class of probability distributions $P(J)$ and later extended by Eggarter *et al.*⁸ to arbitrary probability distributions shows the density of states to exhibit a singularity at zero energy of the form

$$\rho(\epsilon) \sim \frac{1}{\epsilon \ln^3 \epsilon} \tag{1}$$

and consequently, the low-temperature susceptibility

and specific heat behave as

$$\chi(T) \sim \frac{1}{T \ln^2 T/T_0} \tag{2a}$$

$$C(T) \sim \frac{1}{|\ln^3 T/T_0|} \tag{2b}$$

for arbitrary $P(J)$ [except of course $P(J) = \delta(J - J_0)$, or any other form of disorder that can be eliminated by a simple phase transformation⁹]. In Paper I, we found the susceptibility and specific heat of the random Heisenberg chain to behave as

$$\chi(T) \sim 1/T^{\alpha_x(T)} \tag{3a}$$

$$C(T) \sim T^{1-\alpha_c(T)} \tag{3b}$$

with α_x, α_c slowly varying functions of temperature that approach unity as the temperature goes to zero. Clearly, the form [Eq. (2)] can be rewritten as Eq. (3), with

$$\alpha_x(T) = 1 - \frac{2}{\ln T_0/T} \tag{4a}$$

$$\alpha_c(T) = 1 - \frac{3}{\ln T_0/T} \tag{4b}$$

so that a close relation between the XY and Heisenberg model is apparent. [In Eq. (4), we have redefined for convenience $\alpha_x = -d \ln \chi / d \ln T$, which agrees with Eq. (3a) for slowly varying $\alpha_x(T)$, and

similarly for α_c .)]

In this paper we want to shed more light on this relationship by studying the general random anisotropic (Heisenberg-Ising) antiferromagnetic chain [see Eq. (6)]. We consider only the case of a uniform anisotropy, $\gamma = J_z^i/J_x^i$, with J_z^i the i th coupling in the z direction and J_x^i the i th coupling in the xy plane. (A more general model would include the possibility of different anisotropies for different bonds.) $\gamma = 1$ defines the isotropic Heisenberg model, $\gamma = 0$ the XY model, and $\gamma = \infty$ the Ising model. Our model is further defined by the probability distribution for the couplings $P(J_i)$. The couplings for different bonds are taken to be independent random variables.

The method used, which is described in Sec. III, is a numerical implementation of the renormalization-group approach discussed in I, properly extended to the anisotropic case. In I, a further approximation on the recursion relations was made which allowed an approximate analytical evaluation of the renormalized probability distribution $P_n(J)$ for the Heisenberg case. Having an analytic form for $P_n(J)$ gave us a clear physical insight into the qualitative physics of the problem, but the further approximation does lead to small quantitative changes in the results. Here we are interested in more quantitative results and therefore we perform the RG calculation numerically: we generate in the computer a long random chain with couplings obeying a given probability distribution $P(J)$ and perform the iteration procedure numerically with the full recursion relations for the couplings. One could at each step compute the resulting renormalized probability distribution for the couplings but this is not necessary if we only want to obtain the thermodynamic properties. Also, this numerical procedure allows us to study arbitrary probability distributions $P(J)$, and to extend the calculations to the general anisotropic case.

Our results show that in the entire XY region including the Heisenberg point ($\gamma \leq 1$) one obtains singular thermodynamic properties of the form [Eq. (3)] for arbitrary probability distributions. We concentrate on the susceptibility for which better statistics is obtained. We find that the functional form

$$\chi(T) \sim \frac{1}{T |\ln^m T/T_0|} \quad (5)$$

fits our low-temperature numerical results over the whole temperature range studied (about three orders of magnitude), for all values of $\gamma \leq 1$ and arbitrary $P(J)$. T_0 depends strongly on $P(J)$ and γ while m seems to be independent of $P(J)$ and γ and close to two. For the XY model, good agreement is found with Dyson's exact results, which gives us confidence in the reliability of the results for the general $\gamma \neq 0$ case. Since in the XY model $m = 2$, we conjecture this to be a universal result valid for arbitrary $P(J)$ and $\gamma \leq 1$. However, we cannot rule out a possible

weak dependence of m with γ .

In the region $\gamma > 1$, qualitatively different behavior is obtained. Except for the case of a singular probability distribution $P(J)$, there is a gap in the spectrum between the ground state and the first excited states that causes the susceptibility to go to zero at sufficiently low temperatures. However, for sufficiently large randomness and not too large anisotropy the susceptibility shows a divergent approximate power-law behavior over a wide temperature range and only at very low temperatures it goes to zero. Recent experiments¹⁰ on $\text{Qn}(\text{TCNQ})_2$ show the susceptibility to deviate from power-law behavior and turn towards zero at around 5 mK. Even though other explanations are possible, we conclude that a small anisotropy in one direction would be a possible explanation for this effect.

The outline of this paper is as follows: In Sec. II we define the model and review some exact results for it in various limiting cases. In Sec. III we discuss the renormalization-group approach to be used. The method is an extension of a zero-temperature approach¹¹ that has been widely used to study ground-state properties of quantum Hamiltonians. We show how to extend it to make it applicable to compute approximately low-temperature properties. To illustrate the accuracy of the finite-temperature method, we apply it to the uniform Heisenberg chain and compare the results with accurate numerical estimates by Bonner and Fisher.¹² In Sec. IV we obtain the recursion relations for the random chain for arbitrary γ and discuss their behavior qualitatively. From the behavior of the couplings under iterations we can anticipate the low-temperature behavior as a function of γ . In Sec. V we describe the numerical procedure used and show some representative numerical results. Finally we summarize our conclusions in Sec. VI.

II. MODEL

The model of interest is defined by the Hamiltonian

$$H = \sum_i J_i (\sigma_x^i \sigma_x^{i+1} + \sigma_y^i \sigma_y^{i+1} + \gamma \sigma_z^i \sigma_z^{i+1}) + h \sum_i \sigma_z^i, \quad (6)$$

with $0 \leq \gamma < \infty$ and $J_i \geq 0$ a random variable described by a probability distribution $P(J_i)$. σ_x^i , σ_y^i , and σ_z^i are the usual Pauli matrices, and h is an external magnetic field. We will only discuss the thermodynamic properties in the limit $h \rightarrow 0$. Various exact results are known in different limiting cases. For $\gamma = \infty$ (Ising model) the thermodynamic properties in zero magnetic field can be calculated exactly by the transfer matrix technique.^{5,13} One finds for the longitudinal susceptibility

$$\chi = \frac{1}{T} \frac{1 + \langle u \rangle}{1 - \langle u \rangle}, \quad (7)$$

with $u = -\tanh(J_z/T)$. It is easily seen that χ will diverge at low temperatures only if the underlying probability distribution for the couplings is singular: for $P(J_z) \sim 1/J_z^\alpha$, one finds $\chi \sim 1/T^\alpha$. On the other hand, if $P(J_z) = 0$ around $J_z = 0$ the susceptibility will go to zero exponentially at low temperatures. This is of course obvious from a physical point of view since the Ising model will have a nonzero gap if the J_z 's have a lower bound greater than zero. Similarly, for the specific heat one obtains $C(T) \sim T^{1-\alpha}$ if $P(J) \sim 1/J^\alpha$ and C going to zero exponentially if $P(J_z) = 0$ around $J_z = 0$.

For $\gamma = 0$ one obtains the quantum XY model.¹⁴ By using the Jordan-Wigner transformation the Hamiltonian (6) with $\gamma = 0$ can be rewritten as

$$H = \sum_i 2J_i (C_i^\dagger C_{i+1} + C_{i+1}^\dagger C_i), \quad (8)$$

with the operators C_i obeying anticommutation relations. This Hamiltonian, describing free spinless fermion with "off-diagonal disorder," has been extensively studied both numerically¹⁵ and analytically.^{7-9,16} As pointed out by Smith,¹⁶ Dyson⁷ solved many years ago a particular case of a random chain of oscillators that maps onto a Hamiltonian of the form (8). Dyson found an exact solution for the density of states for a particular class of probability distributions of the form

$$P_n(J) = \frac{2n^n}{(n-1)!} \left(\frac{J}{J_0} \right)^{2n-1} e^{-nJ^2/J_0^2}. \quad (9)$$

Note that $P_n(J)$ is nonsingular at the origin and that $P_n(J) \rightarrow \delta(J - J_0)$ as $n \rightarrow \infty$. Nevertheless, from Dyson's exact solution one finds that for any n the density of states at low energies has a singularity of the form

$$\rho(\epsilon) = \frac{1}{\epsilon \ln^3 \epsilon}. \quad (10)$$

This is a rather surprising feature, since for a uniform chain the density of states goes to a constant at the origin. It has been recently shown by Eggarter *et al.*⁸ that the singularity [Eq. (10)] appears universally on the Hamiltonian (8) for *any* randomness present and is not restricted to the particular class of probability distributions [Eq. (9)]. The thermodynamics for the XY chain can be easily obtained from the density of states since it is a free-fermion problem.⁶ One finds for the transverse susceptibility and the specific heat at low temperatures

$$\chi \sim \frac{1}{T \ln^2 T/T_0}, \quad (11a)$$

$$C \sim \frac{1}{|\ln^3 T/T_0|}, \quad (11b)$$

i.e., an arbitrary probability distribution for the cou-

plings produces strong singularities in the density of states and in the thermodynamic properties. For the uniform chain instead, $\chi \rightarrow$ nonzero constant and $C \sim T$ as the temperature goes to zero.

For the case of arbitrary γ , nothing is known exactly for the random case, since the $\sigma_z^i \sigma_z^{i+1}$ term introduces interactions between the fermions and it is now a many-body problem. The Hamiltonian in fermion language is now

$$H = \sum_i [2J_i (C_i^\dagger C_{i+1} + C_{i+1}^\dagger C_i) - 2J_i \gamma C_i^\dagger C_i + 2J_i \gamma (C_i^\dagger C_i)(C_{i+1}^\dagger C_{i+1})]. \quad (12)$$

It has been argued by Theodorou⁵ that the diagonal disorder term $(C_i^\dagger C_i)$ in Eq. (12) should erase the singularity in the density of states [Eq. (10)]. Even though this would be true if the interaction term in Eq. (12) was absent, we will find from our calculation that the interaction term restores a singularity of the same type as occurs for the XY model for the general case $\gamma \leq 1$.

Finally, let us briefly review some results for the uniform Heisenberg-Ising chain, i.e., $P(J) = \delta(J - J_0)$. Various ground-state properties have been calculated exactly from the Bethe-ansatz solution, as well as the form of the low-lying excitations.¹⁷ For $\gamma \leq 1$ the spectrum is gapless and the dispersion law for the elementary excitations goes as $\sin(q)$.¹⁸ Correspondingly, the zero-temperature susceptibility is finite. For $\gamma > 1$ there is a gap in the spectrum and the susceptibility goes to zero exponentially at zero temperature. Ground-state correlation functions have been calculated by Luther and Peschel¹⁹ for a continuum generalization of the Hamiltonian (6). In the region $\gamma \leq 1$, correlation functions decay algebraically with distance with exponents continuously dependent on γ , while for $\gamma > 1$ they decay exponentially. This is to be expected, since there is an exact mapping from this model to the Baxter model²⁰; the region $\gamma \leq 1$ maps onto the line of critical points in the Baxter model. As for finite temperatures, exact results are scarce¹⁷ but there exist reliable finite-cell calculations extrapolated to infinite chains.¹²

In summary, for the uniform chain we find in the entire region $\gamma \leq 1$ qualitatively similar behavior: correlation functions decay algebraically, the spectrum is gapless, and the zero-temperature susceptibility is finite. Hence it will not be too surprising to find in the random chain similar behavior to the random XY model for the entire region $\gamma \leq 1$. Instead, for $\gamma > 1$ in the uniform chain there is a gap and the zero-temperature susceptibility is zero, as in the Ising-model limit. Correspondingly we will find for the random chain that the behavior in that region resembles the one of the random Ising model.

III. RENORMALIZATION-GROUP METHOD

The method used in this work is a simple extension of a zero-temperature RG method¹¹ to make it applicable to study finite-temperature properties. Let H_σ denote the Hamiltonian of a quantum lattice system. We divide the lattice into cells, and the Hamiltonian into an intracell part H_0 and an intercell coupling V :

$$H_\sigma = H_0 + V. \quad (13)$$

The intracell Hamiltonian can be written as a sum of decoupled cell Hamiltonians

$$H_0 = \sum_p H_0^p, \quad (14)$$

where p labels the cells. Each H_0^p has a finite (small) number of degrees of freedom, and can thus be exactly diagonalized. Let $\{l\}_p$ denote a subset of low-lying cell eigenstates for a given cell p , and $\{l\}$ the subset of the Hilbert space formed by products of these low-lying cell states. In the zero-temperature method, one simply truncates the original Hamiltonian to the subspace of state $\{l\}$. The resulting "renormalized Hamiltonian" can usually be cast into the same form as the original one, with "cell operators" replacing the original site operators. Iterating this procedure, one obtains approximate answers for the ground-state properties of the system.

We want to extend this approach to be able to compute approximately finite-temperature properties, with emphasis on low-temperature properties. For that purpose, we write the partition function for the system as

$$Z = \text{Tr}_\sigma e^{-\beta H_\sigma} = \text{Tr}_{\{l\}} e^{-\beta H_\sigma} \left(\frac{\text{Tr}_\sigma e^{-\beta H_\sigma}}{\text{Tr}_{\{l\}} e^{-\beta H_\sigma}} \right). \quad (15)$$

In the first factor, we want to replace H_σ by a renormalized operator that has only matrix elements between the low cell states. We achieve this by introducing a mapping operator $T[\mu|\sigma]$, that maps the low states in σ space to a complete set of states in a smaller Hilbert space μ . $T[\mu|\sigma]$ is defined so that it satisfies

$$\text{Tr}_\mu T[\mu|\sigma] = 1_l, \quad (16)$$

where 1_l denotes the identity in the subspace of σ space spanned by the low-lying cell states. Using Eq. (16), we can then write for the first factor in Eq. (15)

$$\begin{aligned} \text{Tr}_{\{l\}} e^{-\beta H_\sigma} &= \text{Tr}_\mu \text{Tr}_{\{l\}} T[\mu|\sigma] e^{-\beta H_\sigma} \\ &= \text{Tr}_\mu e^{-\beta H_\mu}. \end{aligned} \quad (17)$$

Equation (17) defines the renormalized Hamiltonian H_μ . To lowest order in the intercell coupling, H_μ is simply the original Hamiltonian truncated to the sub-

space of low cell states. In higher order, Eq. (17) takes into account transitions starting at a low cell state, going through intermediate high states and returning to a low state.²¹

The second factor in Eq. (15) we evaluate explicitly to some order in the intercell coupling V . Let

$$\frac{\text{Tr}_\sigma e^{-\beta H_\sigma}}{\text{Tr}_{\{l\}} e^{-\beta H_\sigma}} = e^{-\beta N g}, \quad (18)$$

where N is the number of sites in the system. Combining Eqs. (15), (17), and (18) we obtain for the free energy per site the recursion relation

$$f = g + \frac{1}{s} f', \quad (19)$$

where f' is the free energy per site for the renormalized system, and s is the number of sites per cell. Note that Eq. (19) is of the same form as the usual recursion relation used for classical systems.²²

In a lowest-order calculation, we truncate the Hamiltonian to the subspace of low-lying cell states to obtain H_μ , and compute Eq. (18) to zeroth order in the intercell coupling. We obtain the recursion relation

$$f = -\frac{T}{s} \ln \left[1 + \frac{z_h}{z_l} \right] + \frac{1}{s} f', \quad (20)$$

where z_l and z_h are the cell partition functions for the low- and the remaining higher-lying cell states, respectively,

$$z_l = \text{Tr}_{\{l\}} e^{-\beta H_0^p}, \quad (21a)$$

$$z_h = \text{Tr}_{\{h\}} e^{-\beta H_0^p}. \quad (21b)$$

In this paper, we will restrict ourselves to the lowest-order recursion relation (20). Note that at low temperatures the contributions to the free energy from the first few iterations will be very small (if T is such that $\Delta E/T \gg 1$, with ΔE the gap between the low and high cell states) and only after several iterations one will obtain appreciable contributions in Eq. (20). But at that point one has already included considerable structure in each "supercell" so that the decoupling approximations made are not as drastic as they may seem.

To illustrate the accuracy of the method, we apply it to a uniform Heisenberg chain and compare our results to accurate finite-chain calculations by Bonner and Fisher, extrapolated to infinite chains. We take cells of three sites each and keep only the two lowest-lying states per cell in defining the renormalized Hamiltonian, which is of the same form as the original one. The recursion relations for the general case of arbitrary γ and random J 's will be discussed in the next section. For the particular case of the uniform isotropic Heisenberg chain they are simply $J' = \frac{4}{9}J$, $h' = h$. The partition functions for the cells

are simply calculated from Eq. (21), and the thermodynamic properties are obtained by taking derivatives of Eq. (20).

Figure 1 shows the specific heat from the RG calculation (full line) compared with the Bonner-Fisher (BF) estimate (dashed lines). As expected, the agreement is best at low temperatures, but it is also reasonable at high temperatures, since we have not discarded any of the degrees of freedom in our calculation. We also show in Fig. 1 the specific heat for an anisotropic case ($\gamma = 2$). Here, the specific heat goes to zero exponentially at low temperatures and the maximum shifts to lower values. These features are in agreement with the BF numerical calculations. We do not find the spurious peak at low temperatures that occurs in the BF calculation due to finite-cell effects.

The main defect of this approximate calculation concerns the behavior of the gap. It is known that the gap between the ground state and the first excited state in the AF Heisenberg chain goes as $1/N$, with N the number of sites in the chain. The recursion relation $J' = \frac{4}{9}J$ gives a gap that goes to zero somewhat too slowly (as $1/N^{0.74}$). This is most apparent in the susceptibility: instead of obtaining a susceptibility that goes to a nonzero value at $T = 0$ (which is directly connected to the gap going as $1/N$) we obtain a vanishing zero-temperature susceptibility. In fact, this also causes the specific-heat curve to go to zero with vanishing slope instead of linearly as one expects. However, the slope goes to zero so sharply that it cannot be distinguished in Fig. 1.

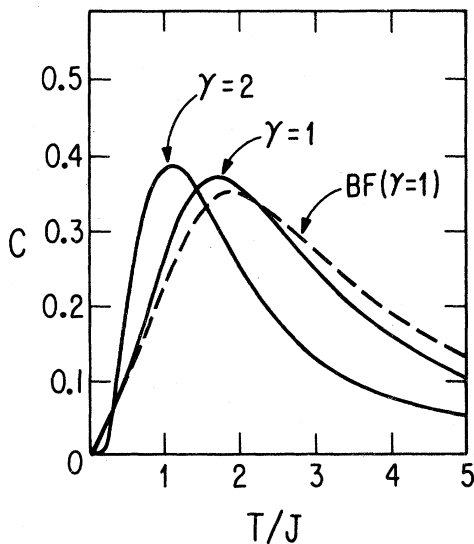


FIG. 1. Specific heat for the isotropic Heisenberg chain ($\gamma = 1$) from the RG calculation (full line) and the Bonner-Fisher calculation (dashed line). Also shown is the specific heat for an anisotropic case ($\gamma = 2$) from the RG calculation.

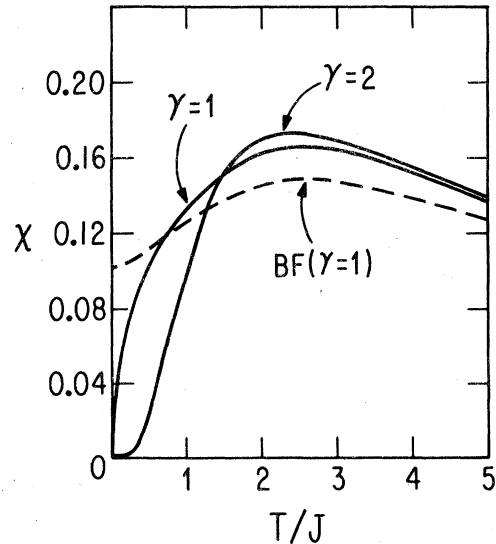


FIG. 2. Susceptibility for the isotropic Heisenberg chain from the RG calculation (full line) and the BF calculation (dashed line). Also shown is the susceptibility for an anisotropic case ($\gamma = 2$) from the RG calculation.

Figure 2 shows the magnetic susceptibility. As expected, the RG curve goes to zero sharply at zero temperature. Nevertheless, the overall agreement with the BF results is reasonably good (the maximum is almost exactly at the same position). As we will argue in Sec. V this inaccuracy at low T for the uniform chain should not affect our conclusions for the random chain. In Fig. 2 we show also the susceptibility for an anisotropic case ($\gamma = 2$): it goes to zero exponentially and the maximum is somewhat shifted and bigger, in agreement with the BF results.

IV. RECURSION RELATIONS

We now proceed to solve the general anisotropic random model. As in the previous section, we divide the chain in cells of three sites, as shown in Fig. 3. Note that we have labeled each bond J_i with a different anisotropy γ_i . The reason is that after the first iteration we will generate different anisotropies for different bonds. Again, we diagonalize the intracell Hamiltonian and keep only the two lowest-lying energy states in each cell. The resulting renormalized Hamiltonian is of the same form as the original one. The recursion relations for the renormalized coupling and anisotropy are (see Fig. 3 for reference)

$$J' = A(J_1, \gamma_1, J_2, \gamma_2)A(J_5, \gamma_5, J_4, \gamma_4)J_3, \quad (22a)$$

$$\gamma' = B(J_1, \gamma_1, J_2, \gamma_2)B(J_5, \gamma_5, J_4, \gamma_4)\gamma_3, \quad (22b)$$

with

$$A = 2a_1 a_2, \quad (23a)$$

$$B = (a_1^2 + a_2^2 - a_3^2) / 2a_1 a_2, \quad (23b)$$

and (a_1, a_2, a_3) the eigenvector corresponding to the lowest eigenvalue of the matrix (for the left cell in Fig. 3)

$$\begin{pmatrix} \gamma_1 J_1 - \gamma_2 J_2 & 2J_2 & 0 \\ 2J_2 & -\gamma_1 J_1 - \gamma_2 J_2 & 2J_1 \\ 0 & 2J_1 & \gamma_2 J_2 - \gamma_1 J_1 \end{pmatrix}. \quad (24)$$

It is interesting to discuss various special cases, where the recursion relations (22) simplify. Consider first the uniform chain (all J_i 's and all γ_i 's equal). The recursion relations simplify to

$$J' = \frac{4a^2}{(2+a^2)^2}, \quad (25a)$$

$$\gamma' = \frac{1}{4} a^2 \gamma, \quad (25b)$$

with

$$a = \frac{4}{(8+\gamma^2)^{1/2} - \gamma}. \quad (26)$$

These recursion relations have been obtained and discussed by Rabin.²³ The Heisenberg point ($\gamma = 1$) is an unstable fixed point. For $\gamma < 1$ the flow is to the XY point $\gamma = 0$. The coupling J and thus the gap between the ground state and first excited state goes to zero in the region $\gamma \leq 1$ as one iterates, in accordance with the known behavior, though somewhat too slowly (as $1/N^{0.74}$ for $\gamma = 1$ and $1/N^{0.63}$ for $\gamma = 0$ instead of as $1/N$). Further, the recursion relations (25) yield the correct algebraic decay of static ground-state correlation functions.²⁴ In the region $\gamma \leq 1$ and the exponents at the Heisenberg and xy points are in good agreement with the known values.^{19,25} However, this simple calculation will not give exponents that vary continuously with γ , since for all $\gamma < 1$ the flow is to the $\gamma = 0$ fixed point and one obtains the XY exponents. A more sophisticated RG calculation that yields a line of fixed point in the region $\gamma \leq 1$ would be needed to reproduce that feature.

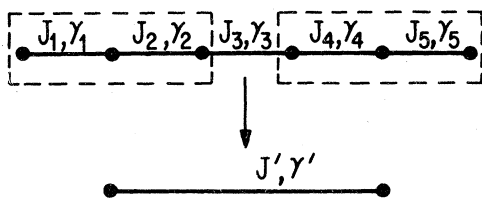


FIG. 3. Three-site cells involved in the RG transformation.

In the region $\gamma > 1$, the flow is to the Ising limit $\gamma = \infty$, and the coupling in the z direction J_z goes to a nonzero value $J_z^\infty > 0$, which indicates a finite gap between the ground state and first excited states. Further, ground-state correlation functions decay exponentially with distance in this region.²⁴ These features are in accordance with the known behavior.

For the disordered case, the points $\gamma_i = 1, 0$, and $\gamma_i = \infty$ for all i are still fixed points of the RG transformation (22). Around the Heisenberg point one obtains (for the left cell of Fig. 3) to first order in $\gamma_1 - 1, \gamma_2 - 1$

$$B(J_1, \gamma_1, J_2, \gamma_2) = 1 + (\gamma_1 - 1)D_1(J_1, J_2) + (\gamma_2 - 1)D_2(J_1, J_2), \quad (27)$$

[see Eq. (22b) for the definition of B], with

$$D_1 = \frac{(3-b)^2}{2b(3+b)} \frac{J_1}{J_1 + J_2 + (J_1^2 + J_2^2 - J_1 J_2)^{1/2}}, \quad (28a)$$

$$D_2 = \frac{b-3}{2b} \frac{J_2}{J_1 + J_2 + (J_1^2 + J_2^2 - J_1 J_2)^{1/2}}, \quad (28b)$$

$$b = \frac{J_1 + J_2 + 2(J_1^2 + J_2^2 - J_1 J_2)^{1/2}}{J_1 - J_2}. \quad (28c)$$

Since $D_1(J_1, J_2)$ and $D_2(J_1, J_2)$ are bigger than zero for all J_1, J_2 Eq. (27) implies that $\gamma_i = 1$ is an unstable fixed point also with disorder. The effect of randomness is only to make the flow away from the fixed point faster than in the uniform case if $J_1 < J_2$ and slower if $J_1 > J_2$.

For the change in the size of the coupling at the Heisenberg point we have, as discussed in I

$$A(J_1, \gamma_1, J_2, \gamma_2) = \frac{2b(b+3)}{3(3+b^2)} = \begin{cases} J_1/2J_2, & J_1 \ll J_2 \\ 1, & J_2 \ll J_1 \\ \frac{2}{3}, & J_1 = J_2. \end{cases} \quad (29)$$

This behavior, in particular, the cases when $J_1 < J_2$, causes the couplings to renormalize to zero exponentially fast on the average, instead of algebraically as occurs in the uniform chain. As discussed in I, this is responsible for the singular behavior of the thermodynamic properties at low temperatures.

Around the XY point we have, to lowest order

$$B(J_2, \gamma_1, J_2, \gamma_2) = \frac{J_1}{(J_1^2 + J_2^2)^{1/2}}. \quad (30)$$

Since $B \leq 1$ for all J_1, J_2 , Eqs. (30) and (22) show that the XY point is a stable fixed point. Again, the effect of randomness is only to make the flow to the XY point faster than in the uniform case if $J_1 < J_2$ and slower if $J_1 > J_2$.

For the change on the size of the couplings at the XY point one obtains

$$A(J_1, J_2) = \frac{J_1}{(J_1^2 + J_2^2)^{1/2}} = \begin{cases} J_1/J_2, & J_1 \ll J_2 \\ 1, & J_2 \ll J_1 \\ 1/\sqrt{2}, & J_1 = J_2. \end{cases} \quad (31)$$

Equation (31) has qualitatively the same behavior as Eq. (29). As a consequence of this, the low-temperature thermodynamic properties at the Heisenberg and XY points will be qualitatively similar.

Finally, let us discuss the recursion relations close to the Ising point. It is convenient to define $\delta = 1/\gamma$ and look at the recursion relations

$$\delta' = D(J_1, \delta_1, J_2, \delta_2) D(J_5, \delta_5, J_4, \delta_4) \delta_3, \quad (32a)$$

$$J'_z = C(J_1, \delta_1, J_2, \delta_2) C(J_5, \delta_5, J_4, \delta_4) J_{z3}. \quad (32b)$$

To lowest order in δ one obtains

$$D(J_1, \delta_1, J_2, \delta_2) = \frac{2J_{z1}}{J_{z2}} \delta_1. \quad (33)$$

Equation (33) shows that the Ising fixed point is stable, since $D < 1$. For $J_{z2} \ll J_{z1}$, the expansion that gives Eq. (33) breaks down and one obtains $D \rightarrow 1$. The effect of randomness on the anisotropy is similar as for the cases discussed earlier. For the change in the coupling size one obtains $C(J_1, \delta_1, J_2, \delta_2) \rightarrow 1$ as $\delta_1, \delta_2 \rightarrow 0$ and this, together with Eq. (32a) will cause the couplings in the z direction to renormalize to finite nonzero values as happens in the uniform case. Hence the thermodynamic properties in this region will be qualitatively different to the ones in the region $\gamma \leq 1$ for sufficiently low temperatures.

Let us summarize the qualitative picture that emerges from these recursion relations. This is most clearly done in terms of the flow diagram in Fig. 4. For simplicity, we consider probability distributions with a cutoff at some $J = J_0$, and characterize the disorder at a given iteration step by the average of the variables $y = -\ln J/J_0$ for the XY region (lower half of Fig. 4) and $y_2 = -\ln J_2/J_0^2$ for the Ising region (upper half) with $J_0^2 = \gamma J_0$. These variables are better behaved statistically than the couplings themselves, as discussed in I. For $\langle y \rangle = 0$ we have the ordered chain $P(J) = \delta(J - J_0)$ and as $\langle y \rangle \rightarrow \infty$ we obtain free spins, and similarly for y_2 . On the vertical axis we plot the average anisotropy $\langle \gamma \rangle$ (although on the axis $\langle \gamma \rangle = 0, 1, \infty$ and $y = 0, y_2 = 0$ we have the same anisotropy for all bonds, i.e., $\gamma_i = \langle \gamma \rangle$ for all i). On the ordered line, the flow is away from the point $\gamma = 1$ as discussed. When we introduce some disorder in the region $\gamma \leq 1$, the flow is to the free-spin limit $\langle y \rangle = \infty$; if $\gamma = 1$ initially this occurs along the $\gamma = 1$ line, if $\gamma < 1$ the flow is also towards the $\gamma = 0$ axis. In either case, it implies that a singularity at the

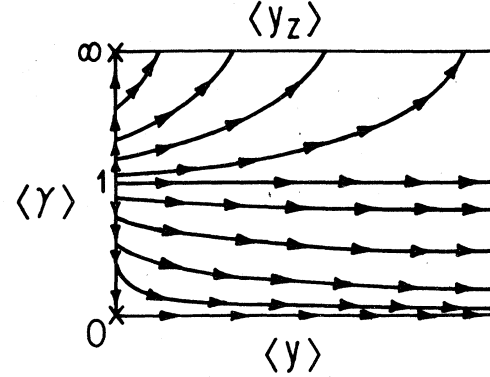


FIG. 4. Flow diagram derived from the recursion relations. On the lower half, the variable on the horizontal axis is $y = -\ln J/J_0$ and in the upper half $y_2 = -\ln J_2/J_0^2$. J_0 is the cutoff in the probability distribution.

origin will be generated in the probability distribution for the couplings after n iterations, $P_n(J)$, for any initial disorder, giving rise to singular thermodynamic behavior at low temperatures. As mentioned earlier, our recursion relations overestimate the flow to the XY limit in the $\gamma < 1$ region (they do not give a "line of fixed points" in the ordered case). Hence, the flow lines in the lower half of Fig. 4 should probably be more "horizontal." For the purposes of this paper however this is not too serious since we will find the thermodynamic behavior in the entire $\gamma \leq 1$ region, including the Heisenberg line, to be quite similar.

In the upper half of Fig. 4, the flow is to the fixed line $\langle \gamma \rangle = \infty$, and the limit $\langle y_2 \rangle = \infty$ is never reached. This implies that if one starts with a nonsingular probability distribution $P(J)$, singularities will not be generated and one will obtain an exponentially vanishing susceptibility and specific heat at low temperature. However, if γ is not too large, the flow to the $\langle \gamma \rangle = \infty$ axis occurs after several iterations and the final $\langle y_2 \rangle$ can be quite large. As we will see in the next section, this implies that there will be an intermediate region in temperature where χ appears to diverge as a power law before it goes to zero at lower temperatures. Qualitatively, for a given temperature range $T_1 < T < T_2$ the susceptibility will be diverging in that interval if we are on a flow line that crosses both lines $\langle y_2 \rangle = -\ln T_1/J_0^2$ and $\langle y_2 \rangle = -\ln T_2/J_0^2$ and will go to zero otherwise.

V. NUMERICAL PROCEDURE AND RESULTS

The free energy is obtained by iterating and averaging Eq. (20), as

$$\bar{f} = -\frac{T}{3} \sum_{n=0}^{\infty} \frac{1}{3} n \left\langle \ln \left[1 + \frac{z_h^{(n)}(T, h)}{z_l^{(n)}(T, h)} \right] \right\rangle. \quad (34)$$

The average $\langle \rangle_n$ is taken with respect to the n th iteration probability distribution $P_n(J)$. In principle, $P_n(J)$ can be obtained from the recursion relations and the starting probability distribution, as discussed in I. However, it looks like a formidable task to compute $P_n(J)$ using the full recursion relations [Eq. (22)], even for the isotropic Heisenberg case. Therefore, in I $P_n(J)$ was evaluated approximately for that case by taking an approximate form for the recursion relations, and the average $\langle \rangle_n$ was calculated by integration. Here, we choose to evaluate Eq. (34) directly by a numerical simulation procedure to avoid any additional approximation on the recursion relations [Eq. (22)]. We generate a long chain of $N = 3^{n_0}$ sites with random couplings distributed according to a given initial $P(J)$ with a given initial γ . We then compute the partition functions for the cells and obtain the first contribution to \bar{f} . Explicitly

$$N\bar{f} = -T \sum_p \ln \left[1 + \frac{z_p^p}{z_1^p} \right] + N'\bar{f}', \quad (35)$$

where p labels cells, and $N' = N/3$. For computing $N'\bar{f}'$ we obtain the new couplings from the recursion relations [Eq. (22)] (we now have a chain with 3^{n_0-1} sites) and repeat this procedure. After a few iterations (say n_1 iterations), if we are in the $\gamma \leq 1$ region all couplings have renormalized to zero (more precisely, to values much less than the given temperature) so that we are left with a chain of $3^{n_0-n_1}$ free spins and can compute their thermodynamics directly. In the Ising region $\gamma > 1$ we are after a few iterations at the Ising point and the thermodynamics of the sites can be computed directly from the transfer matrix formalism. A chain of 3^9 sites was found to be sufficiently long for the temperature range studied (the chain has to be taken longer the lower the temperature). Further, we did the calculations on 8 chains for each case to obtain better statistics.

In Figs. 5 and 6 we show the effect of various degrees of randomness on the specific heat and susceptibility for the Heisenberg case. Qualitatively similar results are obtained in the whole region $\gamma \leq 1$. The probability distribution considered here is of the form

$$P(J) = \theta(J - (1-a))\theta((1+a)-J)/2a, \quad ,$$

i.e., a uniform spread around $J = 1$. For $a \rightarrow 1$, the uniform chain limit is approached. In the specific heat, the effect of the randomness at low temperatures is to yield an infinite slope at zero temperature. This happens for any degree of randomness. At high temperatures, the maximum is broadened and shifted to higher temperatures with respect to the uniform case. For the susceptibility, we see that the disorder causes χ to diverge at low temperatures; for small disorder this happens at lower temperatures but it will occur at sufficiently low temperatures even for "in-

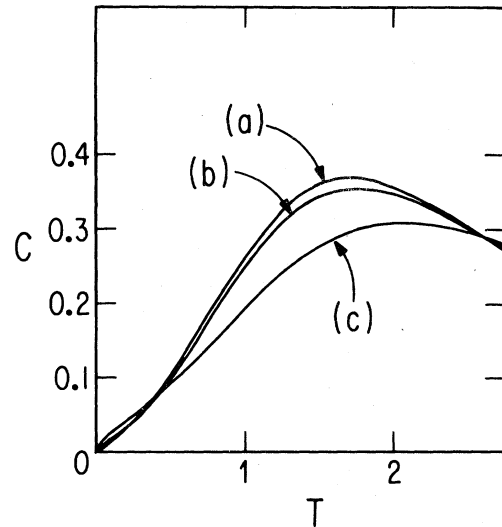


FIG. 5. Specific heat for the isotropic Heisenberg chain with a probability distribution $P(J) = \theta(J - (1-a)) \times \theta((1+a)-J)/2a$. (a) $a = 0$ (uniform chain); (b) $a = 0.5$; and (c) $a = 1$.

finitesimal" disorder. As already mentioned, we somewhat overestimate the gap so that we get a vanishing zero-temperature susceptibility instead of a finite value in the uniform case. Thus, our approximate χ at low temperatures is lower than the true value in that case. If we assume this to still hold in the random case, that would indicate that the susceptibility diverges at least as strongly as found from our approximate calculation.

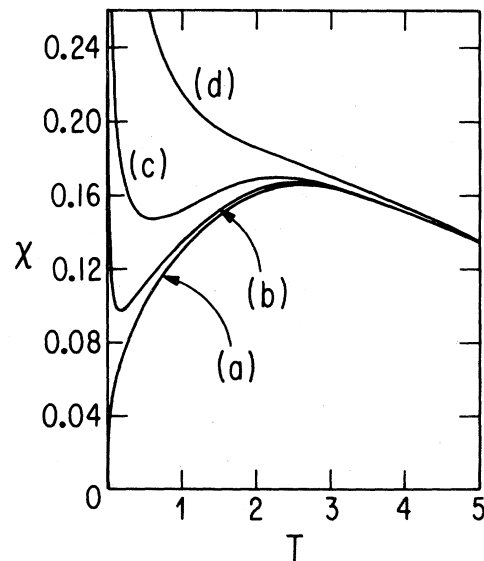


FIG. 6. Susceptibility for the isotropic Heisenberg chain, same probability law as in Fig. 5. (a) $a = 0$; (b) $a = 0.2$; (c) $a = 0.5$; and (d) $a = 1$.

In Figs. 7 we show the specific heat [Fig. 7(a)] and susceptibility [Fig. 7(b)] for a nonsingular probability distribution [$P(J) = \theta(1-J)$] and different values of γ , in a log-log plot versus temperature for the region $\gamma \leq 1$. In this and the following plots we cover a range of three orders of magnitude in temperature, with the highest temperature being about $\frac{1}{30}$ of the average value of the coupling. We see that C and χ show approximate power-law behavior, as found in Paper I, with slopes approaching 0 and 1, respectively, as the temperature is lowered. Very similar behavior is found for any other $P(J)$, whether singular or nonsingular. The thermodynamic quantities show little dependence with γ for $\gamma \leq 1$.

As mentioned in Sec. II, for the XY model we know the exact asymptotic behavior at low temperatures. In particular, for the class of probability distributions discussed by Dyson

$$P_n(J) = \frac{2n^n}{(n-1)!} \left(\frac{J}{J_0}\right)^{2n-1} e^{-n(J^2/J_0)}, \quad (36)$$

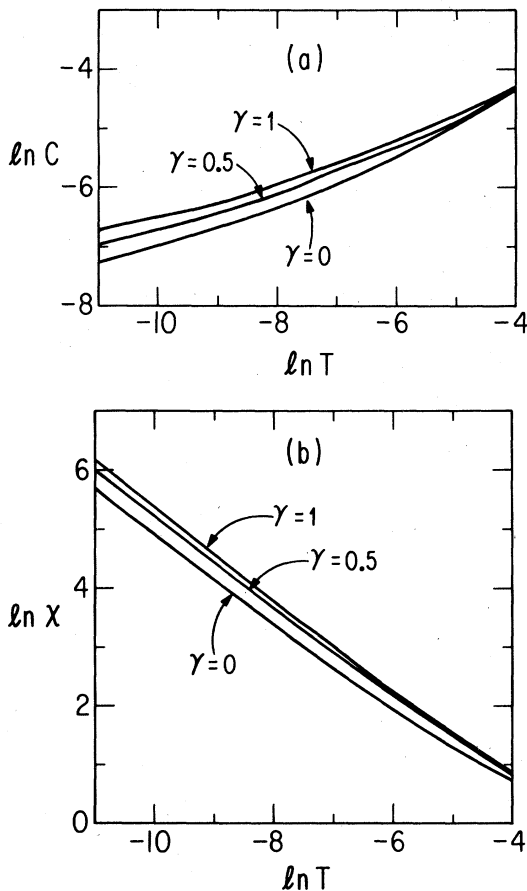


FIG. 7. (a) Specific heat and (b) susceptibility vs temperature (log-log plot) for the probability distribution $P(J) = \theta(1-J)$ and different anisotropies in the region $\gamma \leq 1$.

the low-temperature susceptibility behaves as⁷

$$\chi(T) = \frac{1}{T \ln^2(nT/J_0)} \quad (37)$$

We choose to look at this particular class of $P(J)$'s since here we know the value of the parameter T_0 in Eq. (11a). Of course, this is irrelevant at sufficiently low temperatures but going to too low temperatures would be very computer time consuming. Figure 8 shows the exponent $\alpha_\chi = -d \ln \chi / d \ln T$ for the XY model and the cases $n = 0.2$ and $n = 1$ of Eq. (36) (with $J_0 = 1$). The full lines are the equation obtained from the exact solution (37)

$$\alpha_\chi(T) = 1 - \frac{2}{|\ln nT|} \quad (38)$$

and the empty and full circles the RG calculation for 8 chains of 3^9 sites each (the vertical bars are the standard deviations). Note that there are no adjustable parameters. The agreement is quite satisfactory, considering the simplicity of the approximation used. As n grows, the behavior at a given temperature becomes less singular (α_χ is smaller).

In Fig. 9 we show the exponent α_χ for the probability distributions just discussed and $\gamma = 0.5$ [Fig. 9(a)] and $\gamma = 1$ [Fig. 9(b)]. The behavior is qualitatively similar to the $\gamma = 0$ case. We have fitted our numerical results to a curve of the form

$$\alpha_\chi(T) = 1 - \frac{m}{\ln T/T_0} \quad (39)$$

with $m = 2$ and T_0 an adjustable parameter. T_0 depends strongly on γ and $P(J)$ (for $n = 1$, $T_0 = 8.5$

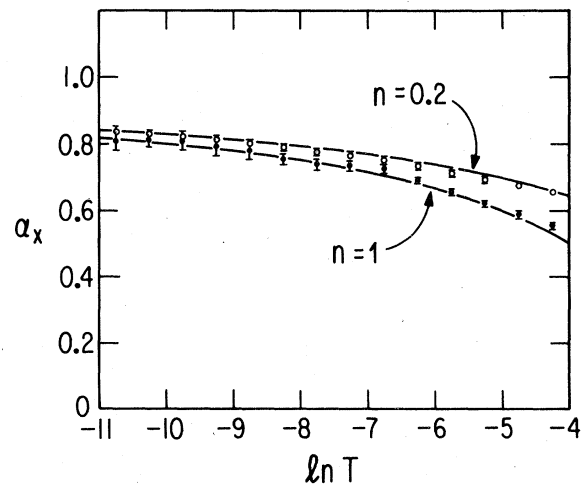


FIG. 8. Susceptibility exponent α_χ vs temperature for the XY model and two probability distributions of the form Eq. (36). The empty and full circles are the RG results for $n = 0.2$ and 1, respectively in Eq. (36), the vertical bars are the standard deviations. The full lines are Dyson's exact solution Eq. (38).

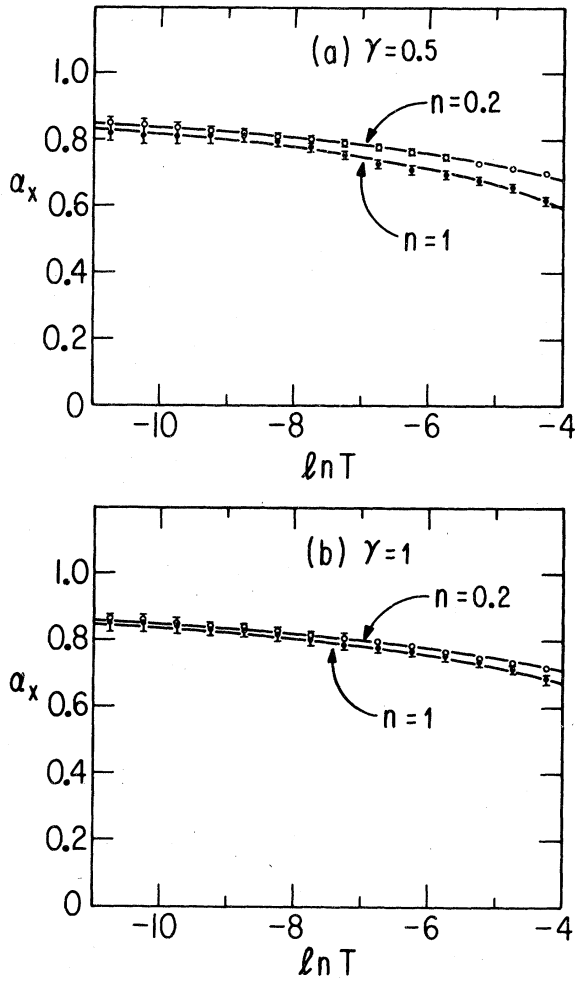


FIG. 9. Susceptibility exponent α_x vs temperature for (a) $\gamma = 0.5$ and (b) $\gamma = 1$ with a probability distribution of the form Eq. (36) and $n = 0.2$ (empty circles) and 1 (full circles). The full lines are Eq. (39) with $m = 2$ and T_0 adjusted to give the best fit.

for $\gamma = 1$, 2.6 for $\gamma = 0.5$ and 1 for $\gamma = 0$ while for $n = 0.2$ $T_0 = 18.9$ for $\gamma = 1$, 9.2 for $\gamma = 0.5$, and 5 for $\gamma = 0$. Comparable fits could be obtained by varying slightly m from 2 and adjusting T_0 accordingly. Even though we cannot rule out a weak dependence of m with γ we conjecture that $m = 2$ is the exact value for all $\gamma \leq 1$ by analogy with the XY model. Of course, an exact argument that proves this would be desirable.

Finally, we show in Fig. 10 the specific heat and susceptibility for $P(J) = \theta(1 - J)$ for various values of γ in the region $\gamma > 1$. For γ not too large, the results are qualitatively similar to the ones obtained in the region $\gamma \leq 1$, i.e., approximately power-law behavior. However, as discussed in the previous section, at sufficiently low temperatures the behavior

changes for any $\gamma > 1$ if the probability distribution is nonsingular, and the susceptibility goes to zero. As we increase γ , the deviations from power-law behavior occur at higher temperature. Recent experiments¹⁰ on the very low-temperature susceptibility of quinolinium (TCNQ)₂ show the susceptibility to deviate from power-law behavior and turn toward zero at around 5 mK. We see from Fig. 10 that some anisotropy in one direction would be a possible explanation for this effect. For different nonsingular probability distributions, the deviations from power-law behavior will occur at different temperatures. For a singular probability distribution instead, one finds singular behavior down to zero temperature since this occurs also in the Ising limit $\gamma = \infty$.

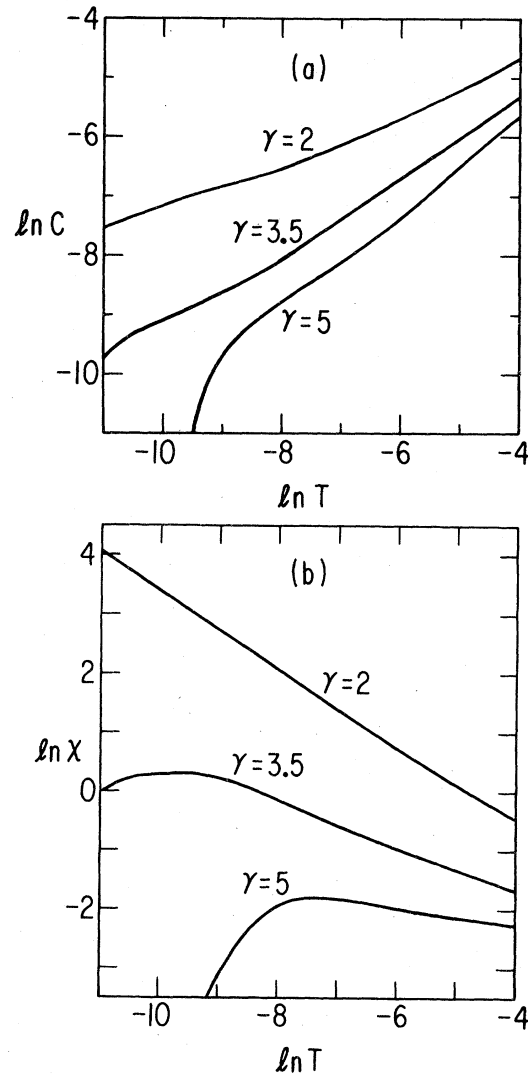


FIG. 10. (a) Specific heat and (b) susceptibility vs temperature (log-log plot) for the probability distribution $P(J) = \theta(1 - J)$ and different anisotropies in the region $\gamma > 1$.

VI. SUMMARY AND CONCLUSIONS

We have performed a numerical renormalization-group study of the low-temperature properties of a random Heisenberg-Ising antiferromagnetic chain. For the Heisenberg case, the results were already anticipated from the analytic results in I: any disorder in the couplings will produce singular thermodynamic properties at low temperatures. For the entire XY region, including the Heisenberg point, the low-temperature susceptibility was found to be of the form $\chi \sim 1/T \ln^m(T/T_0)$ for arbitrary randomness. At the XY point, m is known to be 2 exactly and T_0 depends on the underlying probability distributions; in particular, for the class of probability distributions studied by Dyson T_0 is known exactly as a function of $P(J)$. We compared our numerical results with these exact results at the XY point and found good agreement. For $\gamma \neq 0$, we fitted our result for the susceptibility to the above form with $m = 2$ and found that T_0 depended strongly on $P(J)$ and on γ . Comparable fits to the ones discussed can be obtained with m in the range 1.5 to 2.5 but not beyond, adjusting T_0 accordingly, for all cases studied. Although we cannot rule out a possible weak dependence of m with γ , we conjecture $m = 2$ to be a universal result in the region $0 \leq \gamma \leq 1$ for arbitrary $P(J)$.

In the Ising region ($\gamma > 1$) it was found that the susceptibility goes to zero at sufficiently low temperatures for a nonsingular probability distribution, as happens in the Ising limit $\gamma = \infty$. However, for not too large anisotropy it was found that the susceptibility shows an approximate power-law divergence over a wide range of temperatures and only turns towards zero at very low temperatures. These results resemble very recent experimental results on $\text{Qn}(\text{TCNQ})_2$, where χ is found to deviate from power-law behavior and turn towards zero at around 5 mK. We conclude therefore that some anisotropy in one direction would be a possible explanation for this effect.

ACKNOWLEDGMENTS

I am grateful to G. Mazenko for helpful discussions, for his encouragement, and for reading the manuscript and making helpful comments. Stimulating conversations with J. V. Jose are also acknowledged. I have also benefitted from conversations with M. H. Cohen, W. G. Clark, C. M. Gould, and R. Orbach. This work was supported by the Materials Research Laboratory program of the National Science Foundation at the University of Chicago. In addition, the author was supported by a Victor A. Andrew Memorial Fellowship.

*Submitted in partial fulfillment of the requirements for a Ph.D. degree in the Department of Physics, University of Chicago.

[†]Present address: Institute for Theoretical Physics, University of California, Santa Barbara, Calif. 93106.

¹J. E. Hirsch and J. V. Jose, *J. Phys. C* **13**, L53 (1980), and (unpublished).

²G. Theodorou and M. H. Cohen, *Phys. Rev. Lett.* **37**, 1014 (1976).

³W. G. Clark and L. C. Tippie, *Phys. Rev. B* **20**, 2914 (1979).

⁴S. Ma, C. Dasgupta, and S. Hu, *Phys. Rev. Lett.* **43**, 1434 (1979).

⁵G. Theodorou, *Phys. Rev. B* **16**, 2264 (1977).

⁶L. N. Bulavskii, A. V. Zvarykina, Y. S. Karimov, R. B. Lyubovskii, and L. F. Shchegolev, *Sov. Phys. JETP* **35**, 348 (1972).

⁷F. J. Dyson, *Phys. Rev.* **92**, 1331 (1953).

⁸T. P. Eggarter and R. Riedinger, *Phys. Rev. B* **18**, 569 (1978).

⁹G. Theodorou and M. H. Cohen, *Phys. Rev. B* **13**, 4597 (1976).

¹⁰H. M. Bozler, C. M. Gould, T. J. Bartolac, W. G. Clark, K. Glover, and J. Sanny, *Bull. Am. Phys. Soc.* **25**, 217 (1980).

¹¹S. D. Drell, M. Weinstein, and S. Yankielowicz, *Phys. Rev. D* **16**, 1769 (1977).

¹²J. C. Bonner and M. E. Fisher, *Phys. Rev.* **135**, A640 (1964).

¹³D. Cabib and S. D. Mahanti, *Prog. Theor. Phys.* **51**, 1030 (1974).

¹⁴E. Lieb, T. Schultz, and D. Mattis, *Ann. Phys. (N.Y.)* **16**, 407 (1961).

¹⁵M. Weissman and N. V. Cohan, *J. Phys. C* **8**, L145 (1975).

¹⁶E. R. Smith, *J. Phys. C* **3**, 1419 (1970).

¹⁷See J. C. Bonner, *J. Appl. Phys.* **49**, 3 (1978), and references therein.

¹⁸J. des Cloizeaux and M. Gaudin, *J. Math. Phys.* **7**, 1384 (1966).

¹⁹A. Luther and I. Peschel, *Phys. Rev. B* **12**, 3908 (1975).

²⁰R. J. Baxter, *Ann. Phys. (N.Y.)* **70**, 373 (1972).

²¹J. E. Hirsch and G. F. Mazenko, *Phys. Rev. B* **19**, 2656 (1979).

²²T. Niemeijer and J. M. J. van Leeuwen, in *Phase Transitions and Critical Phenomena*, edited by C. Domb and M. S. Green (Academic, New York, 1976), Vol. 6, p. 425.

²³J. M. Rabin (unpublished).

²⁴J. E. Hirsch (unpublished).

²⁵B. McCoy, *Phys. Rev.* **173**, 531 (1968).